A Journal of the Gesellschaft Deutscher Chemiker

Angewandte International Edition GDCh Chemie

www.angewandte.org

Accepted Article

Title: Nucleation and Growth Mechanism of Anion-Derived Solid Electrolyte Interphase

Authors: Chong Yan, Li-Li Jiang, Yu-Xing Yao, Yang Lu, Jia-Qi Huang, and Qiang Zhang

This manuscript has been accepted after peer review and appears as an Accepted Article online prior to editing, proofing, and formal publication of the final Version of Record (VoR). This work is currently citable by using the Digital Object Identifier (DOI) given below. The VoR will be published online in Early View as soon as possible and may be different to this Accepted Article as a result of editing. Readers should obtain the VoR from the journal website shown below when it is published to ensure accuracy of information. The authors are responsible for the content of this Accepted Article.

To be cited as: *Angew. Chem. Int. Ed.* 10.1002/anie.202100494

Link to VoR: https://doi.org/10.1002/anie.202100494

WILEY-VCH

10.1002/anie.202100494

WILEY-VCH

COMMUNICATION

Nucleation and Growth Mechanism of Anion-Derived Solid Electrolyte Interphase

Chong Yan, Li-Li Jiang, Yu-Xing Yao, Yang Lu, Jia-Qi Huang, Qiang Zhang*

Abstract: Solid electrolyte interphase (SEI) has been widely employed to describe the new phase formed between anode and electrolyte in working batteries. Significant advances have been achieved on the structure and composition of SEI as well as on the possible ion transport mechanism. However, the nucleation and growth mechanism of SEI catches little attention, which requires the establishment of isothermal electrochemical crystallization theory. Herein we explore the virgin territory of electrochemically crystallized SEI. By using potentiostatic method to regulate the decomposition of anions, an anion-derived SEI forms on graphite surface at atomic scale. After fitting the cur-rent-time transients with Laviron theory and Avrami formula, we conclude that the formation of anion-derived interface is surface reaction controlled and obeys the two-dimensional (2D) progressive nucleation and growth model. Atomic force microscope (AFM) images emphasize the conclusion, which reveals the mystery of isothermal electrochemical crystallization of SEI.

The development of rechargeable batteries facilitates our mobile life and efficiently assists to become global carbon-neutral.[1] Among all components of batteries, electrode materials and electrode/electrolyte interfaces are always mentioned in the same breath, inseparable like shadows.[2, 3] When an electrode operates beyond the stability window of electrolytes, which is widely accepted that a solid electrolyte interphase (SEI) forms at the electrode/electrolyte interface and dictates the performance of the working devices.[4, 5] The investigation of SEI is still a challenging topic till today,[6] and fortunately significant advances have been made on the structure [7] and composition of SEI [8]as well as on the ion transport mechanism.[2, 9]

However, as a first-order phase transition that produces nanoscale crystalline products at the electrode/electrolyte interface, the nucleation and growth mechanism of SEI has always been a mystery. The scenario focuses on the formation theory is an un-cultivated land that has not been reported yet. In addition, the SEI is difficult to characterize because of its rapid manner of formation, air sensitivity and fragility against high-energy photon/electron beam.[10, 11] Therefore, the crystallographic mechanism of SEI needs to be carefully studied, which may guide the design of SEI with desired properties.

Note that the solvation structure of electrolyte dominates the interface properties of a battery.[2, 5] Different electrolyte systems with distinct solvation structures are chosen as model systems in this work (**Figure 1a**), including routine concentration electrolyte (RCE),[12, 13] high concentration electrolyte (HCE),[14-16] localized high concentration electrolyte (LHCE) [17, 18]and weakly-solvating electrolyte (WSE).[19] Ethylene carbonate (EC) or other strongly-solvating solvents completely occupy the inner solvation sheath in RCE,[13] while anions can replace parts of solvents to appear in the inner solvation sheath of HCE, LHCE, and WSE by electrostatic ion-pairing interactions.[16, 17, 19] In general, the species that participate in the inner solvation sheath will be preferentially reduced to form SEI. It has been reported that EC solvent occupies the inner solvation layer and preferentially gets reduced, the decomposition potential of EC solvent in RCE is around 0.8 V versus Li/Li$^+$.[20] Compared with organic solvents, anions involved in the solvation structure are electrochemically reduced at higher potentials to form anion-derived SEI.[11] The mechanism of polycrystalline SEI induced by solvents or anions needs to be explored in-depth.[19]

In this contribution, an anion-derived SEI layer was generated on electrode surface through a potentiostatic method. By controlling the decomposition of anions and inhibiting the decomposition of solvents at atomic scale, an inorganic-rich polycrystalline of SEI was identified. After fitting the as-obtained current-time transients with the Laviron theory [21, 22] and the Avrami formula,[23, 24] we find that surface reduction reaction concerns exclusively the adsorbed species, and the formation mechanism of anion-derived interface obeys two-dimensional (2D) progressive nucleation and growth model. These results reveal the mystery of isothermal electrochemical crystallization model of SEI.

Graphite electrode was employed as the substrate for studying nucleation and growth behavior of SEI due to the low chemical reactivity and few side reactions. Two types of voltage curves are obtained in typical electrolyte systems (**Figure 1b**). The potential of graphite abnormally rebounds to a higher value in HCE, LHCE, and WSE under galvanostatic discharge condition, forming a voltage pit. However, it does not happen in RCE (**Figure 1c**). The formation of such a voltage pit is a typical sign of nucleation overpotential. That is, an additional driving force for anion-derived SEI formation is needed to deposit nanoscale nuclei on the working electrode in HCE, LHCE, and WSE, leading to the sudden increase of working potential. It is still a mystery whether the nuclei will occur when EC is reduced on the electrode, because the responding signal can not be detected effectively.

[a] C. Yan, Y.-X. Yao, Y, Lu, Prof. Q. Zhang
Beijing Key Laboratory of Green Chemical Reaction Engineering and Technology, Department of Chemical Engineering
Tsinghua University
Beijing 100084 (P.R. China)
E-mail: zhang-qiang@mails.tsinghua.edu.cn
[b] Prof. J.-Q. Huang
Advanced Research Institute of Multidisciplinary Science
Beijing Institute of Technology
Beijing 100081 (P.R. China)
[c] Dr. L.-L. Jiang
Key Laboratory for Special Functional Materials in Jilin Provincial Universities, Jilin Institute of Chemical Technology
Jilin 132022 (P.R. China)

Supporting information for this article is given via a link at the end of the document.

Accepted Manuscript

This article is protected by copyright. All rights reserved.

10.1002/anie.202100494

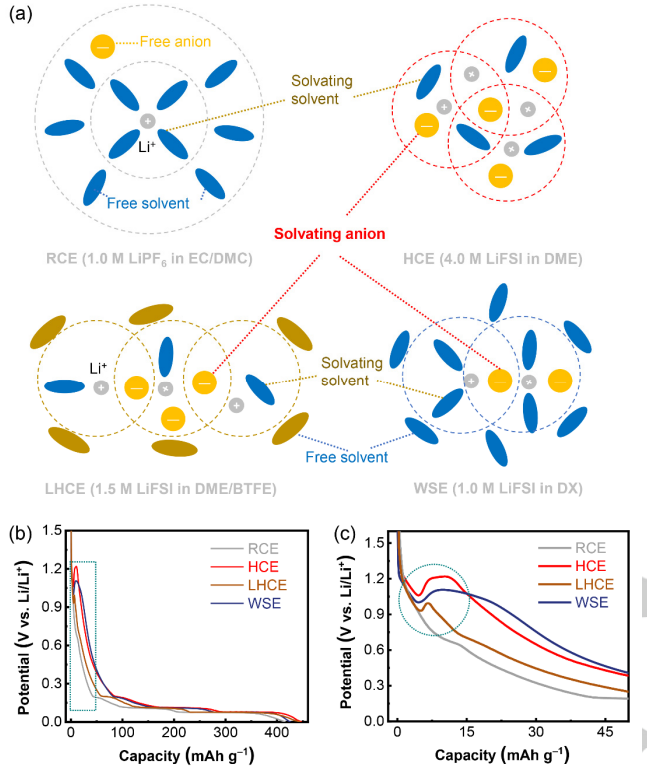

Figure 1. The diagram of solvation structure and the electrochemical performance. (a)The ion-solvents solvation sheaths of RCE, HCE, LHCE and WSE. (b) The capacity-potential plots of the 1st cycle in Li | graphite batteries. (c) is the enlarged drawing of the dashed box in (b), the dashed cycle in (c) exhibits the abnormal potential-rebounded phenomenon.

The compositions of raw graphite electrode (**Figure S1**) and anion-derived SEI on graphite were characterized by X-ray photoelectron spectroscopy (XPS). By comparing the SEI formed in HCE (**Figure S2**), LHCE (**Figure S3 and S4**), and WSE (**Figure S5**), we conclude that the chemical components of SEI in different electrolyte systems remain similar. The spectra of C 1s is from the graphite electrode, and the spectra of F 1s is generated from the LiF (684.8 eV) and PVDF binder (688.3 eV). Li_2O (528.0 eV), Li_3N (397.5 eV), and Li_2S (161.1 eV) are all confirmed in the spectra of O 1s, N 1s and S 2p (**Figure S1-5**). The inorganic products originate from the decomposition of FSI^-, which has been reported in previous studies.[14, 25] The results identify that the interface covering graphite is dominated by the reduction of anions in HCE, LHCE, and WSE. In order to clearly investigate the formation mechanism of SEI, this work employs WSE as the key object of research.

The abnormal phenomenon indicates a special electrochemical reaction has taken place at the three-phase boundary of graphite electrode, SEI, and electrolyte. Cyclic voltammetry was employed to investigate whether the feedback is surface reaction controlled or interface diffusion controlled. A positive linear relation between the reduction peak current and scanning rate is established, confirming that the surface adsorbed species dominate the reaction on graphite surface (**Figure S6**).[25] Therefore, Laviron theory (1)[22] is obeyed and the number of transfer electrons (n) is calculated to be 1.84, evidencing a two-electron reduction path of FSI^-. The analysis above is based on the following equation:

$$i_p=n^2F^2AT_Tv/4RT=nFQv/4RT \quad (1)$$

where i_p is the current peak, F is the Faraday constant, A is the reaction area of electrode, Q is the charges, T is the experimental temperature, n is the transfer electrons and v is the scan rate.

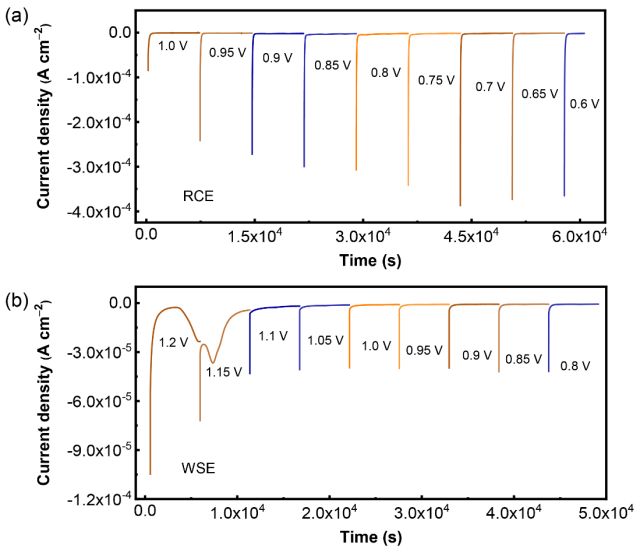

Figure 2. The PITT measurements of Li | graphite batteries. (a) The response current with the gradient decreased potential near the reduced potential of EC and (b) FSI^- in RCE and WSE.

Potentiostatic intermittent titration technique (PITT) with a 0.05 V interval was further used to study the details of the abnormal voltage-rebounding phenomenon. This technique allows us to determine the overpotential needed to trigger the nucleation process. For RCE, there is no additional signal from 1.0 to 0.6 V (**Figure 2a**), but it is easy to observe the rising current in WSE from 1.2 to 1.1 V (**Figure 2b**). The rising current is attributed to the nucleation and growth of crystals occurred at the three-phase boundaries on graphite electrodes. Moreover, the generated nanocrystals possess poor affinity with the organic electrolytes, presenting a high surface energy barrier that must be overcome. The results are well consistent with the potential-rebounding phenomenon. It is worth mentioning that the responding current peak has not been detected in RCE, which does not represent the absence of nucleation and growth for solvent-derived SEI. It may be a result of to the strong affinity between SEI and electrolytes.

Therefore, potentiostatic method was selected to control the specific decomposition of anions (FSI^-) and inhibit the decomposition of solvents, which expects to harvest an anion-derived SEI on graphite surface.

The corresponding current and potential plots versus time are presented in **Figure 3a**. An obvious nucleation and growth peak was detected. We plot $(I/I_m)^2$ against t/t_m and fit it with the theoretical formulae (Equation (2), (3), (4), (5)) of progressive (P) / instantaneous (I) nucleation by 2D (BFT model) [26] or 3D (SH model) growth mechanisms:[27] Herein, BFT represents Beweick, M. Fleischman, and H.R. Thirsk; SH represents Scharifker-Hills.

$$j/j_m=(t/t_m)\exp\{1/2\,[(1-(t/t_m)^2]\} \quad (2,2DI)$$

$$j/j_m=(t/t_m)^2\exp\{2/3\,[1-(t/t_m)^3]\} \quad (3,2DP)$$

$$j/j_m=(1.9542\,t_m/t)^{1/2}\{1-\exp[1.2564t/t_m]\} \quad (4,3DI)$$

$$j/j_m=(1.2254\,t_m/t)^{1/2}\{1-\exp[2.3367\,(t/t_m)^2]\} \quad (5,3DP)$$

This article is protected by copyright. All rights reserved.

Accepted Manuscript

10.1002/anie.202100494

where j_m is the maximal peak and t_m is derived from the maximum at time $t=t_m$.

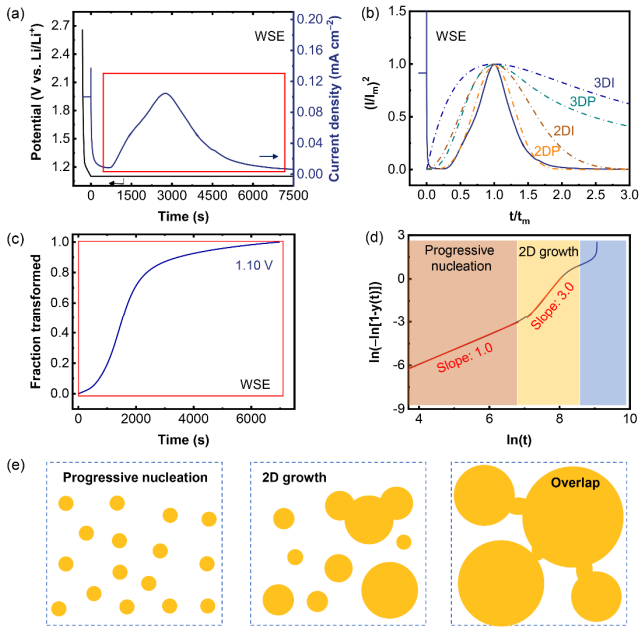

Figure 3. The 2D progressive nucleation and growth of the anion-derived SEI. (a) the potential and current plot versus time for a Li | graphite battery with WSE. (b) The t/t_m and $(I/I_m)^2$ plots (solid line) in comparison with theoretical 2D and 3D models. (c) The fraction transformation of the SEI versus time after normalization. (d) Avrami plot after fitting the enclosed part in (c). (e) The schematic diagram of the 2D progressive nucleation and growth at the three-phase boundary between graphite, SEI and electrolyte.

The obtained results are well-consistent with progressive nucleation and 2D growth (**Figure 3b**). The $(I/I_m)^2$ increases rapidly at the beginning and finally approaches zero, representing a self-limiting growth regime.

In addition, a normalized sigmoidal cumulative function and the fitting data were exhibited in **Figure 3c** according to the Avrami formula (Equation (6)):[24]

$$Y=1-\exp(-Bt^n) \qquad (6)$$

where Y is the fraction of the materials has been transformed, B is a kinetic constant, n is the Avrami exponent.

An Avrami exponent of 1.0 at the beginning and 3.0 at the middle-posterior segment are observed (**Figure 3d**), further evidencing the progressive nucleation and 2D growth.[28] Therefore, the nucleation and growth model of anion-induced SEI can be described as the scenario (**Figure 3e**): the SEI formation is dominated by surface reaction (reduction of FSI^- here), and the electron transfer number is 2. The number of nucleation sites increases progressively, and each nucleus undergoes 2D growth before overlapping with others. Only when the whole electrode surface is completely covered by reduced products, an ion-conducting but electron-insulating polycrystalline film forms, which marks the end of SEI growth.

When the electro-crystallization was finished, subsequent intercalation of Li ions into graphite can follow (**Figure S7a**). Expectedly, the potential-rebounded phenomenon disappears (**Figure S7b**) due to the existence of an SEI. The post-galvanostatic curve perfectly overlaps with the original one below 0.8 V (**Figure S7c**). The result emphasizes that the anion-induced SEI has been completely formed at 1.10 V and there is no extra electrodeposition of SEI below 0.8 V. Moreover, the nucleation and growth process of SEI will contribute about 5% capacity of the battery (**Figure S7b**), which helps to quantitatively explain why the intercalation capacity of graphite always exceeds the theoretical specific capacity (372 mAh g^{-1}) in the first cycle.

Electrochemical impedance spectroscopy (EIS) was obtained to evaluate the trends in SEI resistance during formation process. The results demonstrate that the resistance of electrode is reduced during SEI nucleation and growth (**Figure S8**). By employing the distribution of relaxation times (DRT) analysis,[29] we find the decrease of SEI resistance is the dominate factor (**Figure S9**), which is attributed to the increase of SEI ionic conductivity and compact feature. In addition, it is also found that the reduction amplitude of resistance is synchronous with the response current. The rapid increased current corresponding to the sharp reduced resistance (**Figure S8b,h**) while the almost constant current lead to the slight change of resistance (**Figure S8c,i**). This confirms the electrochemical crystallization process of electrode can be regulated by the potentiostatic deposition time.

The electrodeposition rate of SEI highly depends on the over-potential of electrodes (**Figure S10**). Note that the high driving force of the electrode can overcome the surface nucleation energy barrier, accelerating the SEI formation and shorten the maximal duration to reach current peak. The transformed data (**Figure S11**) of t/t_m and $(I/I_m)^2$ at 1.08 and 1.04 V also confirmed 2D progressive nucleation and growth after comparison with theoretical models. When we raise the potential of the electrode to 1.24 V, the nucleation and growth time of SEI has obviously increased, and the number of responding peaks is 4 (**Figure S12**), probably corresponding to the multilayer 2D growth of SEI.[30] The influence on the thickness and structure of polycrystalline SEI formed under different over-potentials will be involved in the future work.

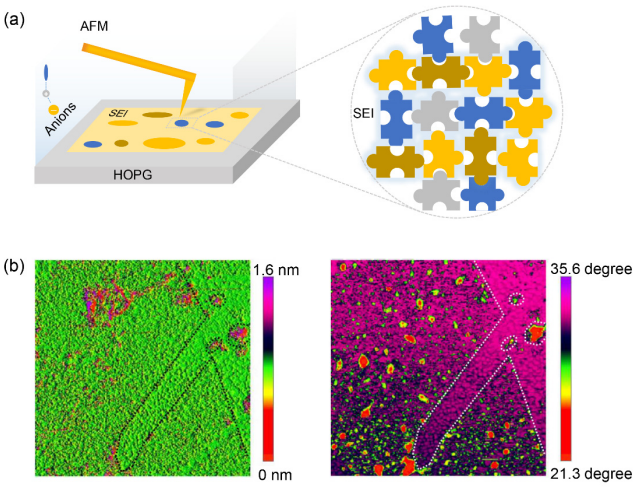

Figure 4. The AFM ex situ studies for the anion-derived SEI. (a) The schematic diagram of the AFM measurement on HOPG and the SEI of mosaic structure in WSE. (b) The AFM height and phase images of transient SEI formed on HOPG.

Furthermore, the nucleation and growth of anion-derived SEI is investigated by atomic force microscopy (AFM) with highly oriented pyrolytic graphite (HOPG) as the substrate (**Figure 4a**). When control the fraction of the transformed crystals to about 55% (**Figure S13**), so that both the nucleation sites, 2D growth flakes and blank areas can be observed (**Figure 4b**). The thickness

This article is protected by copyright. All rights reserved.

Accepted Manuscript

amplitude of the HOPG is about 1.6 nm, indicating there is insufficient space to accommodate the 3D growth of products. Therefore, the results of AFM enhanced the 2D progressive nucleation and growth model of SEI. The SEI is mainly composed of inorganic compounds (including Li_2O, LiF, Li_2S, Li_3N, *etc.*) and exhibits a mosaic structure.

There are at least three design principles that need to be considered when controlling the nucleation and growth of SEI on electrodes. Firstly, the electrochemical reduction potential of anions must be higher than that of solvents. The reduction potential mentioned here takes into account the influence of solvation. Secondly, the reduced products should have poor solubility and weak affinity with electrolyte, which ensure that the corresponding signal can be detected from the electrochemical curves and facilitate to start, pause and terminate the nucleation and growth process of SEI. Thirdly, the overpotential applies on the electrode should not be high. The high over-potential hardly ensures the complete decomposition of species, and the strong driving force can cause the out-of-order stacking of crystals.

In summary, we report the electrochemical crystallization behavior of SEI for the first time. The nucleation and growth behavior of anion-derived SEI on graphite electrode is revealed by classical crystallographic theories, demonstrating a 2D progressive nucleation and growth regime. The results explore an uncultivated land of SEI and the methodology here can be extended to the investigation of SEI on other anode materials (silicon, lithium metal, zinc, *etc.*). The conclusion of this contribution takes a major step toward the understanding of isothermal electrochemical crystallization theory of SEI, which exhibits huge potential in designing controllable interfaces in rechargeable batteries.

Acknowledgements

This work was supported by National Natural Science Foundation of China (21825501 and 51702117), National Key Research and Development Program (2016YFA0202500), Tsinghua University Initiative Scientific Research Program, Department of Science and Technology of Jilin Province (20180520014JH). C. Yan and Y. Lu appreciates the Shuimu Tsinghua Scholar Program of Tsinghua University, and National Postdoctoral Program for Innovative Talents (BX20200176). The authors thank discussion with Xiang Chen, Rui Xu, Wenlong Cai and Lei Xu.

Keywords: solid electrolyte interphase • nucleation and growth mechanism • two-dimension (2D) growth • interfacial chemistry • isothermal electrochemical crystallization

[1] M. Winter, B. Barnett, K. Xu, *Chem. Rev.* **2018**, *118*, 11433-11456; W. L. Cai, Y. X. Yao, G. L. Zhu, C. Yan, L. L. Jiang, C. X. He, J. Q. Huang, Q. Zhang, *Chem. Soc. Rev.* **2020**, *49*, 3806-3833.

[2] C. Yan, R. Xu, Y. Xiao, J.-F. Ding, L. Xu, B.-Q. Li, J.-Q. Huang, *Adv. Funct. Mater.* **2020**, *30*, 1909887.

[3] L. Suo, O. Borodin, T. Gao, M. Olguin, J. Ho, X. Fan, C. Luo, C. Wang, K. Xu, *Science* **2015**, *350*, 938-943; C. Yan, H. Yuan, H. S. Park, J.-Q. Huang, *J. Energy Chem.* **2020**, *47*, 217-220; C. Yan, Y. Yao, W.-L. Cai, L. Xu, S. Kaskel, H. S. Park, J. Huang, *J. Energy Chem.* **2020**, *49*, 335-338.

[4] E. Peled, *J. Electrochem. Soc.* **1979**, *126*, 2047-2051.

[5] K. Xu, *Chem. Rev.* **2014**, *114*, 11503-11618.

[6] M. Gauthier, T. J. Carney, A. Grimaud, L. Giordano, N. Pour, H.-H. Chang, D. P. Fenning, S. F. Lux, O. Paschos, C. Bauer, F. Maglia, S. Lupart, P. Lamp, Y. Shao-Horn, *J. Phys. Chem. Lett.* **2015**, *6*, 4653-4672.

[7] D. Aurbach, *J. Power Sources* **2000**, *89*, 206-218; Y. Li, Y. Li, A. Pei, K. Yan, Y. Sun, C. L. Wu, L. M. Joubert, R. Chin, A. L. Koh, Y. Yu, J. Perrino, B. Butz, S. Chu, Y. Cui, *Science* **2017**, *358*, 506-510; B. Li, X. Chen, X. Chen, C. Zhao, R. Zhang, X. Cheng, Q. Zhang, *Reserach* **2019**, *2019*, 4608940; Y. Yao, X. Zhang, B. Li, C. Yan, P. Chen, J. Huang, Q. Zhang, *InfoMat* **2020**, *2*, 379-388; X. Shen, X. Cheng, P. Shi, J.-Q. Huang, X. Zhang, C. Yan, T. Li, Q. Zhang, *J. Energy Chem.* **2019**, *37*, 29-34; C. Yan, X.-B. Cheng, Y. Tian, X. Chen, X.-Q. Zhang, W.-J. Li, J.-Q. Huang, Q. Zhang, *Adv. Mater.* **2018**, *30*, 1707629.

[8] C. Yan, H.-R. Li, X. Chen, X.-Q. Zhang, X.-B. Cheng, R. Xu, J.-Q. Huang, Q. Zhang, *J. Am. Chem. Soc.* **2019**, *141*, 9422-9429.

[9] S. Shi, P. Lu, Z. Liu, Y. Qi, L. G. Hector, Jr., H. Li, S. J. Harris, *J. Am. Chem. Soc.* **2012**, *134*, 15476-15487.

[10] X. Cao, X. Ren, L. Zou, M. H. Engelhard, W. Huang, H. Wang, B. E. Matthews, H. Lee, C. Niu, B. W. Arey, Y. Cui, C. Wang, J. Xiao, J. Liu, W. Xu, J.-G. Zhang, *Nat. Energy* **2019**, *4*, 796-805.

[11] Y. Yamada, J. H. Wang, S. Ko, E. Watanabe, A. Yamada, *Nat. Energy* **2019**, *4*, 269-280.

[12] K. Xu, Y. Lam, S. S. Zhang, T. R. Jow, T. B. Curtis, *J. Phys. Chem. C* **2007**, *111*, 7411-7421; A. von Cresce, K. Xu, *Electrochem. Solid-State Lett.* **2011**, *14*, A154-A156.

[13] A. von Wald Cresce, O. Borodin, K. Xu, *J. Phys. Chem. C* **2012**, *116*, 26111-26117.

[14] L. Suo, Y. S. Hu, H. Li, M. Armand, L. Chen, *Nat. Commun.* **2013**, *4*, 1481.

[15] J. Qian, W. A. Henderson, W. Xu, P. Bhattacharya, M. Engelhard, O. Borodin, J. G. Zhang, *Nat. Commun.* **2015**, *6*, 6362.

[16] Y. Yamada, K. Furukawa, K. Sodeyama, K. Kikuchi, M. Yaegashi, Y. Tateyama, A. Yamada, *J. Am. Chem. Soc.* **2014**, *136*, 5039-5046.

[17] S. Chen, J. Zheng, D. Mei, K. S. Han, M. H. Engelhard, W. Zhao, W. Xu, J. Liu, J.-G. Zhang, *Adv. Mater.* **2018**, *30*, 1706102.

[18] J. Zheng, S. Chen, W. Zhao, J. Song, M. H. Engelhard, J.-G. Zhang, *ACS Energy Lett.* **2018**, *3*, 315-321.

[19] Y.-X. Yao, X. Chen, C. Yan, X.-Q. Zhang, W.-L. Cai, J.-Q. Huang, Q. Zhang, *Angew. Chem. Int. Ed. in*doi: 10.1002/anie.202011482.

[20] S. Zhang, M. S. Ding, K. Xu, J. Allen, T. R. Jow, *Electrochem. Solid-State Lett.* **2001**, *4*, A206-A208; L. Wang, A. Menakath, F. Han, Y. Wang, P. Y. Zavalij, K. J. Gaskell, O. Borodin, D. Iuga, S. P. Brown, C. Wang, K. Xu, B. W. Eichhorn, *Nat. Chem.* **2019**, *11*, 789-796.

[21] Nicholson, S. R., *Anal. Chem.* **1965**, *37*, 1351-1355.

[22] E., Laviron, *J. Electroanal. Chem. Interfacial Electrochem.* **1974**, *52*, 395-402; E. Laviron, *J. Electroanal. Chem. Interfacial Electrochem.* **1974**, *52*, 355-393; E. Laviron, *J. Electroanal. Chem.* **1979**, *101*, 19-28.

[23] R. F. M. William A. Johnson, Member A.I.M.E, *Trans. Am. Inst. Min. Metall. Eng.* **1939**, *135*, 416-442.

[24] M. Avrami, *J. Chem. Phys.* **1939**, *7*, 1103-1112; M. Avrami, *J. Chem. Phys.* **1940**, *8*, 212-224; M. Avrami, *J. Chem. Phys.* **1941**, *9*, 177-184.

[25] L. L. Jiang, C. Yan, Y. X. Yao, W. Cai, J. Q. Huang, Q. Zhang, *Angew. Chem. Int. Ed.* doi: 10.1002/anie.202009738.

[26] A. Bewick, M. Fleischmann, H. R. Thirsk, *Trans. Faraday Soc.* **1962**, *58*, 2200-2216.

[27] B. Scharifker, G. Hills, *Electrochim. Acta* **1983**, *28*, 879-889; Z. Li, Y. Zhou, Y. Wang, Y.-C. Lu, *Adv. Energy Mater.* **2019**, *9*, 1802207.

[28] A. Milchev, I. Krastev, *Electrochim. Acta* **2011**, *56*, 2399-2403; F. Y. Fan, W. C. Carter, Y. M. Chiang, *Adv. Mater.* **2015**, *27*, 5203-5209.

[29] M. Steinhauer, S. Risse, N. Wagner, K. A. Friedrich, *Electrochim. Acta* **2017**, *228*, 652-658; X. Zhou, J. Huang, Z. Pan, M. Ouyang, *J. Power Sources* **2019**, *426*, 216-222; J. P. Schmidt, T. Chrobak, M. Ender, J. Illig, D. Klotz, E. Ivers-Tiffée, *J. Power Sources* **2011**, *196*, 5342-5348.

[30] M. Fleischmann, H. R. Thirsk, *J. Electrochem. Soc.* **1963**, *110*, 688-698; W. Obreten, D. Kashchiev, V. Bostanov, *J. Cryst. Growth* **1989**, *96*, 843-848; D. Kashchiev, *J. Cryst. Growth* **1977**, *40*, 29-46.

This article is protected by copyright. All rights reserved.

Accepted Manuscript

10.1002/anie.202100494

WILEY-VCH

COMMUNICATION

The nucleation and growth behavior of anion-derived SEI on graphite electrode is revealed, the number of nucleation sites increases progressively, and each nucleus undergoes 2D growth before overlapping with others. Only when the whole electrode surface is completely covered by reduced products, an ion-conducting but electron-insulating polycrystalline film forms, which marks the end of SEI growth.

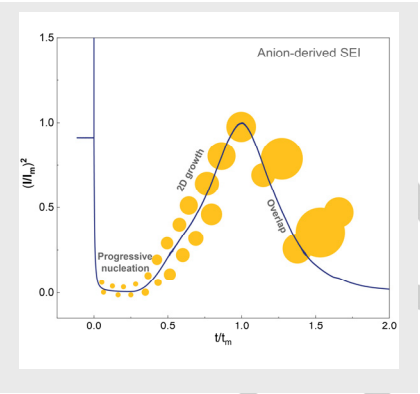

*Chong Yan, Li-Li Jiang, Yu-Xing Yao, Yang Lu, Jia-Qi Huang, Qiang Zhang**

Page No. – Page No.

Nucleation and Growth Mechanism of Anion-Derived Solid Electrolyte Interphase

WILEY-VCH

Accepted Manuscript

This article is protected by copyright. All rights reserved.